Proceedings of Ninth World Conference on Earthquake Engineering
August 2-9, 1988, Tokyo-Kyoto, JAPAN (Vol.IV)

6-1-16

EXPERIMENTAL STUDY ON SEISMIC BEHAVIOR OF TWO-STORIED SOPHISTICATED MODEL FOR NUCLEAR REACTOR BUILDING USING PSEUDO DYNAMIC TESTING METHOD

Kazuhide SATO , Akira HIGASHIURA and Takahito YANASE

Engineering Research Institute,
Sato Kogyo Co., Ltd.,
47-3, Sanda, Atsugi, Kanagawa 243-02 Japan

SUMMARY

In this paper, the authors present the investigation on the seismic behaviors of a nuclear reactor building by the pseudo dynamic testing method. First, the psuedo dynamic testing method is formulated by employing substructuring technique. Second, the specimen, which is subjected to the computer controlled lateral static loading, and the test results obtained by this experiment are discribed. Third, discussions are made about the test results in detail; the authors find that it is possible to simulate the dynamic response of the building under severe earthquake excitation by the pseudo dynamic testing method.

INTRODUCTION

A BWR-type nuclear reactor (BNR) building consists of the structural elements such as box walls, truncated conical walls, etc. As the seismic behavior of such a building is complicated, it is very difficult to perform a lateral loading test of whole building to estimate load-deflection characteristics. Moreover, since the shape and reinforcement of those walls are different from earthquake resistant walls used in an ordinary structure, it is indispensable to carry out experimental studies on those walls to determind the load-deflection characteristics for the BNR building. The satisfactory load-deflection characteristic models for a dynamic analysis of those complicated structure have not been sufficiently revealed.

In this paper, the authors present the results of investigations into the seismic behavior of a BNR building using the pseudo dynamic testing (PDT) method which employs substructuring techniqe.

PSEUDO DYNAMIC TESTING METHOD

The PDT method (Ref. 1), a kind of the earthquake simulation analysis, is a relatively new experimental technique for the evaluation of the performance of complete structural elements subjected to seismic excitations. The PDT method employs substructuring technique (Ref. 2); it combines experiment and numerical analysis so as to make use of the benefits of both techniques. By the substructuring technique, the building is divided into two parts: experimental part and analytical lumped-mass model. The stiffness of the former part is not

predetermined becouse it exhibit nonlinear, hence measured directly from the specimen subjected to using lateral loads, while that of the later part is predetermined becauce they behave elastically. To evaluate the initial stiffness of the specimen, the pretest by lateral static loads is carried out. The equations of motion of the whole structure (Responce Analysis System is shown in Fig. 1) having appropriate viscous dumping are solved numerically using the measured stiffness by direct integration step-by-step algorithms. The procedure is repeated to determine the seismic behavior of the building. In the real time static loading test to estimate the stiffness of the specimen, lateral load are controlled by computer using earthquake ground motion. Newmark's beta method (beta=1/4) is adopted for numerical integration.

RESPONSE ANALYSIS SYSTEM

The PDT method employs the substructuring technique to simulate the seismic behavior of the BNR building. In this experiment, the BNR building is divided into upper and lower parts to facilitate use of the substructuring technique. The upper part is a experimental part and the lower part is an analytical part. Fig. 1 describes the RAN system, for a typical BNR building.

The RAN system for the PDT method using the substructuring technique takes the following into consideration.

1. The numerical part of the BNR building, which is 18M high from its base, is assumed to be a single-stick lumped-mass (SSLM) model.
2. The top of the building which extends up to 50.5m is not considered in the RAN system as the stiffness and mass are much lesser than that of lower part.
3. The experimental part is combined mathematically with the numerical part in the RAN system by considering the compatibility conditions for forces and displacements.
4. The stiffness of the experimental part is measured directly from the specimen with the static lateral loading.
5. Soil-structure interaction is considered in the RAN system. The RAN system is set on supporting ground, the shear wave velocity Vs of which is 1000m/sec.

The properties of the RAN system are listed in Table 1 and the natural period of the RAN system and the SSLM model, is listed in Table 2. Since the RAN system is different in those numerical models to the SSLM model, the natural period of the RAN system is 0.01 sec. less than that of the SSLM model. The synthetic earthquake ground motion is shown in Fig. 2. The maximum acceleration is 452.5 gal.

TEST SPECIMEN AND LOADING PROCEDURE

The specimen, which is a model of the experimental part of the BNR building, is a two-storied and half-symmetrical sophisticated model composed of box and truncated conical walls. The scale of speicemen is about one twentyfifth. Details and properties of the specimen are shown in Fig. 3 and listed in Table 3. Thickness for the walls and slabs are 8cm and 5cm, respectively. The reinforcement ratio for the box wall is 1.2%, while that of the truncated conical wall at the base of the 1st and 2nd stories is 1.5% and 1.8%, respectively. The material properties the concrete and the steel reinforcing bar are listed in Table 4.

The test set up is illustreted in Fig. 4. Lateral static loads are applied to each slab using four computer controlled actuators with servomechanism. A constant axial stress of 20kg/cm^2 is applied uniformly over the closs-section area

at the base of each walls. To approximate the boundary conditions of the specimen with those of the full shaped model, the devices for preventing torsion are placed on the specimen as illustrated in Fig. 5. The deflections and the deformations of the specimen, and the strain of the reinforcing bars and concrete on the surface, are automatically obtained.

RESULTS OF EXPERIMENT AND DISCUSSIONS

Displacement time history in node 1, 2, 3 and 4 of the RAN system are shown in Fig. 6. Maximum displacement at the top of the RAN system, which is the average of nodes 1 and 2, occurred at 5.21 sec. Displacement of the truncated conical wall (node 3) is about 1.8 times the maximum displacement of the box wall (node 1). The relationship between the shear force and the relative displacement of each storied are shown in Fig. 7. Maximum shear force of the 1st and 2nd story of the specimen is 56.3 tonf and 38.8 tonf, respectively. The crack distribution pattern of the specimen at the end of loading is illustrated in Fig. 8. Some shear clacks are obserbed on the web of both the box and truncated conical walls at the 1st story.

Maximum response displacement are computed by the numerical procedure using single-stick and three-sticks lumped-mass model in order to compare the results of the experiment. A comparison between the maximum displacements obtained from the RAN system and the numerical procedures are shown in Fig. 9. Maximum displacements obtained by the pseudo dynamic test are equivalent to those obtained by that models using the approximate earthquake ground motion.

To investigate changes in the properties of the specimen during the experiment, the maximum displacement at the top of the RAN system is evaluated using the moving window Fourier spectrum technique (Ref. 3) illustrated in Fig. 10. In the final stage of the experiment, the natural period of the system increased about 1.5 times as long as that in elastic region.

Following the pseudo dynamic test, the lateral static loading is applied to the specimen in order to investigate the load-deflection relationship. The maximum shear strength of the specimen obtained by the lateral static loading test is 169.4 tonf, which was about three times obtained by the pseudo dynamic test.

CONCLUSION

The results obtained by the pseudo dynamic test are as follows:

1. The maximum displacements obtained by this experiment are equivalent to those obtained by the numerical procedure using the approximate earthquake ground motion.
2. The displacement of the truncated conical wall of the specimen is about 1.8 times that of the box wall.
3. In the final stage of the experiment, the natural period of the RAN system is increased to about 1.5 times that of the elastic region.
4. Some shear cracks are observed in the web of the walls on the 1st and 2nd stories.
5. The maximum shear strength of the test specimen obtained by the PDT is about one third of its ultimate shear strength.

We find that the PDT method is an effective testing method to estimate the seismic behaviors of a complicated struture like this specimen.

ACKNOWLEDGEMENT

The study presented herein is one of experimental works conducted in series under advices of a technical research committee organized in Building Research Promotion Association, Tokyo, Japan. The authors are indebted to members of the Committee for their valuable discussion.

REFERENCES

1. Sato, K., Higashiura, A., Tsutsumi, H., Suzuki, T., and Kondo, G. "A proposed pseudo-dynamic test system.(part 1- 4).," summaries of technical papers at annual meeting of the Architectural Institute Japan, 1985 (in Japanese).
2. Sato, K., Higashiura, A., Yanase, T., and Watanabe, S., "Experimental study on seismic behavior of sophisticated two-storied model of nuclear reactor building, " Proceedings of the 7th Japan Earthquake Engineering Symposium 1986 (in Japanese).
3. Kubo, T., "Simulation of three-dimensional strong earthquake ground motions (Part 2)., " Transactions of Architectural Institute of Japan, No.268, 1978 (in Japanese).

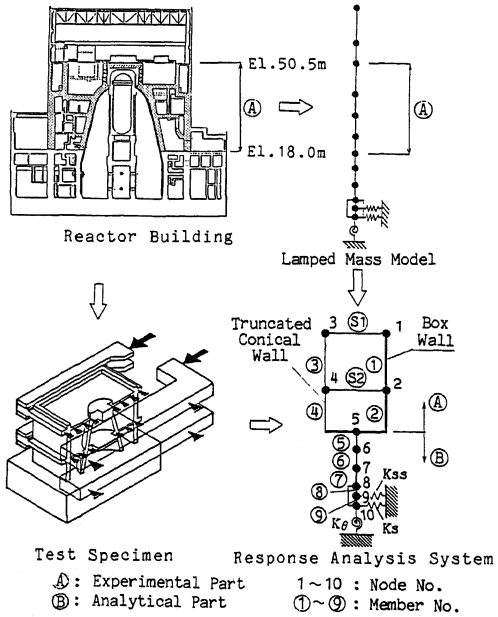

Fig. 1 Modeling of A Typical BWR-type Nuclear Reactor Building

Table 1 Properties of Response Analysis System

Member Number	Effctive Shear Area ($\times 10^4$ mm^2)	Area Moment of Inetia ($\times 10^{10}$ mm^4)
1	10.49	7.48
2	17.66	12.17
3	5.16	1.02
4	8.73	2.09
5	47.85	56.97
6	50.07	61.63
7	50.07	61.63
8	505.60	426.10
9	505.60	426.10

Node Number	Mass (tf sec^2/mm)	Mass Moment of Inertia (tf sec^2 mm/rad.)
1	8.91×10^{-5}	——
2	8.33×10^{-5}	——
3	5.83×10^{-5}	——
4	4.97×10^{-5}	——
5	1.53×10^{-4}	1.29×10^{2}
6	1.14×10^{-4}	0.96×10^{2}
7	1.02×10^{-4}	0.86×10^{2}
8	0.0	0.0
9	4.07×10^{-4}	3.46×10^{2}
10	0.0	0.0

Spring Number	Spring Constant	Damping Factor
Kss	4.176×10^{2}tf/mm	10.0%
Ks	7.226×10^{2}tf/mm	20.0%
K	1.624×10^{9}tf mm/rad.	7.5%
S1	18.61tf/mm	5.0%
S2	17.72tf/mm	5.0%

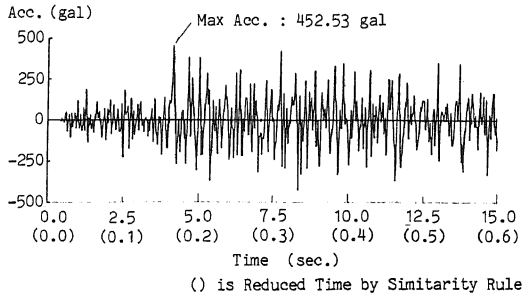

() is Reduced Time by Simitarity Rule

Fig. 2 Input Ground Motion

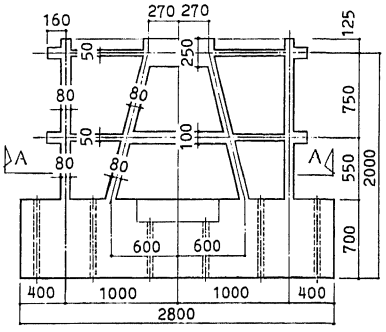

Elevation

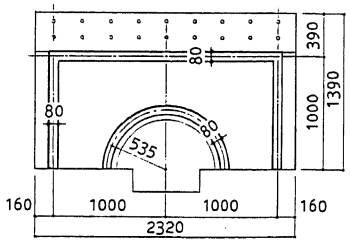

A-A Section

Fig. 3 Shape of Specimen

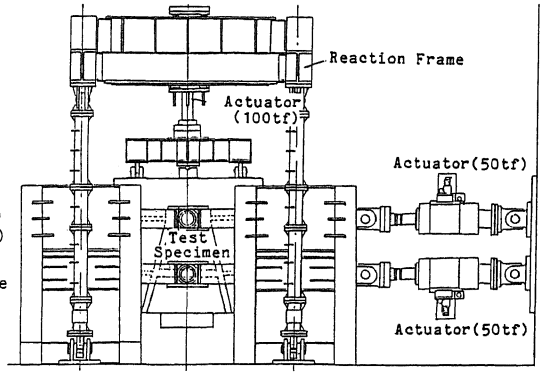

Fig. 4 Test Set Up

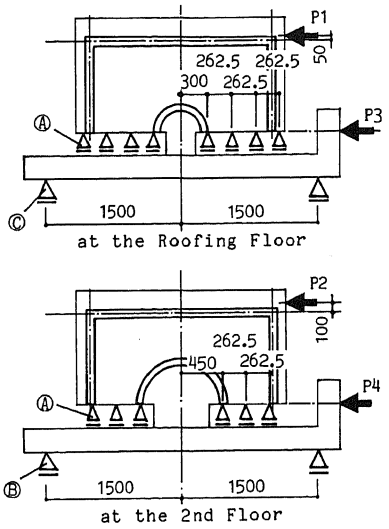

Ⓐ,Ⓑ,Ⓒ : Device for Restrictions of Torsional Motion

Fig. 5 Loading Condition

Table 2 Comparison of Natural Period

Mode	Single Stick Lumped mass Model	Response Analysis System
1	0.2734	0.2625
2	0.1211	0.1760
3	0.0866	0.1535
4	0.0682	0.1105
5	0.0530	0.0785

Table 4 Characteristics of Materials

Concrete

Compression Strength (kgf/cm^2)	Young's Modulas ($x10^5 kgf/cm^2$)	Poison's Ratio
278	1.59	0.17

Steel Reinforcement

Yield Strength (kgf/cm^2)	Tensile Strength (kgf/cm^2)	Young's Modulas ($x10^6 kgf/cm^2$)
4454	5735	1.98

Table 3 Properties of Specimen

Type		BWR Mark Ⅱ
Scale		1/25
Height h		550mm (2nd Floor)
		1350mm (Roofing Floor)
Box Wall	Span L	2000mm
	h/L	0.65
	Thickness t	80mm
	Reinforcement Ratio pw	1.5%
Truncated Conical Wall	Radius r	600mm (Base)
		460mm (2nd Floor)
		270mm (Roofing Floor)
	h/2r	1.08
	Thickness	80mm
	Reinforcement Ratio pw	1.5% (Base)
		1.8% (2nd Floor)
Slab	Thickness	50mm
	Reinforcement Ratio pg	1.4% (Longitudinal)
		1.7% (Transverse)
Axial Stress		$20kgf/cm^2$

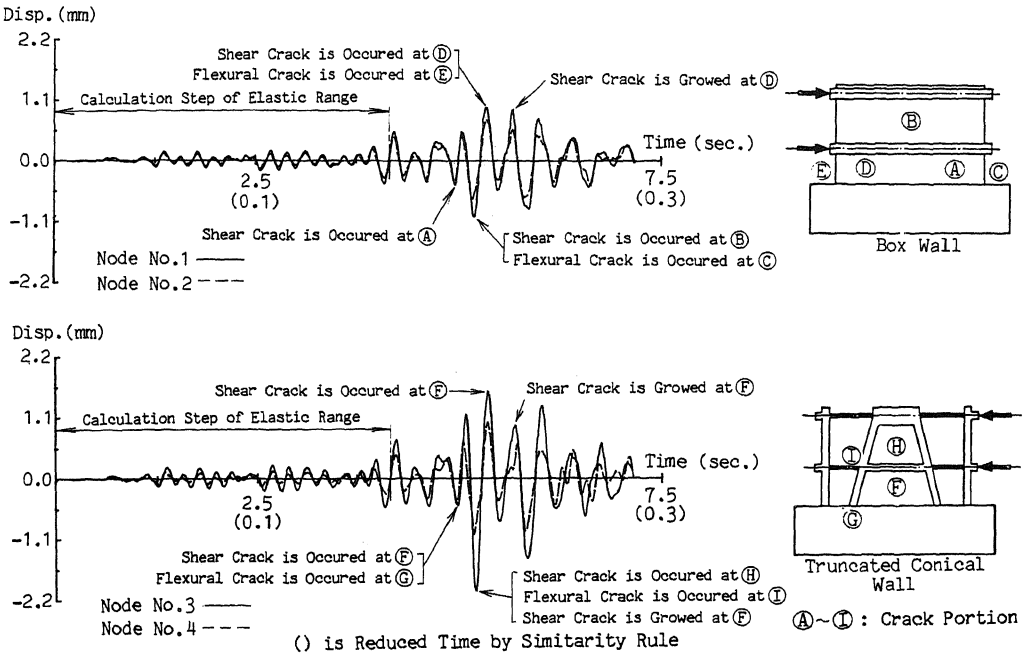

Fig. 6 Time History of Displacement in Node 1, 2, 3, and 4

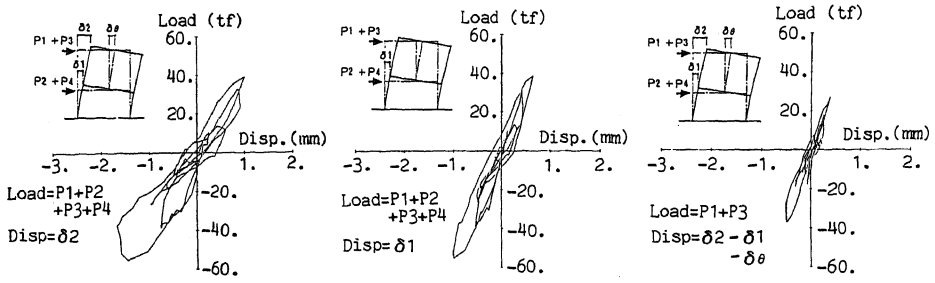

Fig. 7 Relationship Between Shear Force and Relative Displacement

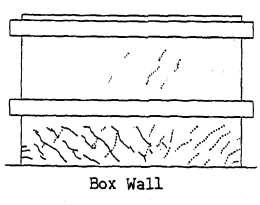

Fig. 8 Crack Pattern

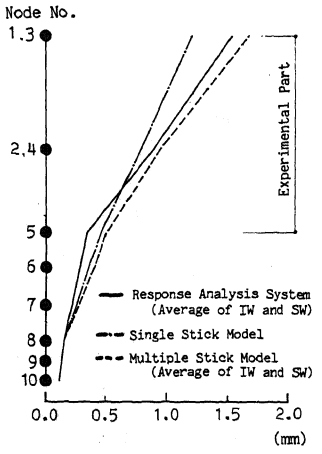

Fig. 9 Comparison of Maximum Displacement

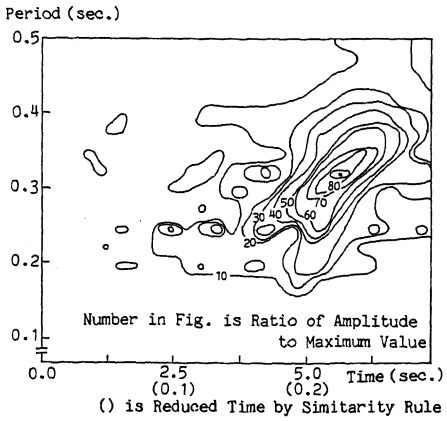

Fig. 10 Moving Window Fourier Spectrum